ACS APPLIED MATERIALS & INTERFACES

Research Article

www.acsami.org

Hydrogen Passivation of Impurities in Al_2O_3

Minseok Choi,*[,†,‡] Anderson Janotti,[†] and Chris G. Van de Walle[†]

[†]Materials Department, University of California, Santa Barbara, California 93106, United States

[‡]Advanced Characterization & Analysis Group, Korea Institute of Materials Science, Changwon 642-831, Korea

ABSTRACT: Carbon and nitrogen are contaminant impurities in Al_2O_3 dielectrics grown by atomic layer deposition, leading to deleterious effects in device performance. We investigate whether these impurities can be passivated using hydrogen. The role of atomic hydrogen in the electronic properties is addressed by examining formation energies and charge-state transition levels of C−H and N−H complexes. Combined with calculated band alignment, we then assess the impact on Al_2O_3/semiconductor interfaces. We find that hydrogen is indeed an effective passivating agent: it removes carbon-related carrier traps and passivates negative fixed charge associated with nitrogen.

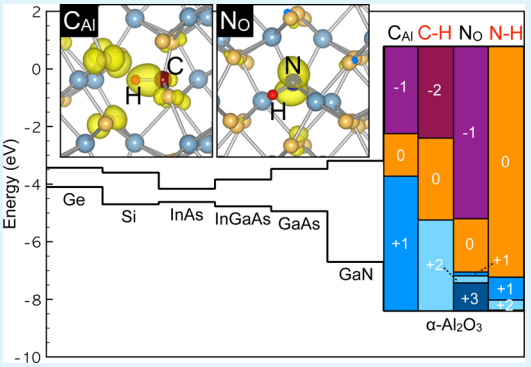

KEYWORDS: *metal-oxide-semiconductor structure, leakage currents, dielectrics, impurities, passivation, hydrogen*

INTRODUCTION

Al_2O_3 is a technically important material for a variety of applications: as a substrate for epitaxial growth,[1] as a support of metal-based catalysts for CO_2 hydrogenation,[2] and as a surface passivation layer of Si solar cells.[3] Impurity-doped Al_2O_3 is widely used in optical devices, for instance, Cr- or Ti-doped sapphire lasers, and C- or Mg-doped crystals are employed in optical data storage and luminescence detection of ionizing radiation.[4] Recently, Al_2O_3 has emerged as a promising gate dielectric for novel electronic devices. Higher-*k* dielectrics to replace SiO_2 in metal-oxide-semiconductor (MOS) devices are pursued to meet requirements in device scaling. Concurrently, channel materials are being investigated for applications in high-power switching devices (using III-nitrides)[5−7] and high-speed, low-power field-effect transistors (using Ge and III-arsenides).[6,8] Promising results have been achieved with Al_2O_3 as the gate dielectric, resulting in devices that exhibit relatively low interface-state densities.[6,7,9−11] However, the performance of such devices is still limited, mainly due to the presence of carrier traps and fixed charges at or near the interface, the microscopic nature of which is still under investigation.

The observed carrier traps and fixed charges in oxide/semiconductor structures have typically been attributed to intrinsic point defects in the dielectric.[9,12−15] First-principles calculations for defects in Al_2O_3 indeed indicate that oxygen vacancies behave as carrier traps, while other native point defects act as fixed charges.[16−18] However, unintentional impurities in the oxide may also play an important role. Most of the oxide dielectrics are grown by atomic layer deposition (ALD), and impurities such as carbon and nitrogen are often incorporated, probably due to incomplete decomposition of ALD precursors.[19−21] Experiments have pointed to carbon as a cause of leakage current in HfO_2/Si MOS structures since leakage current correlates with carbon concentration in the HfO_2 layer.[22,23] The presence of carbon in Al_2O_3 synthesized by ALD was confirmed by atom-probe tomography.[24] Carbon has also been suggested as the culprit for slow trap states near Al_2O_3/GaN interfaces grown by metal−organic chemical vapor deposition (MOCVD).[25,26] First-principles calculations also indicate that carbon impurities easily incorporate on the Al site (C_{Al}) and lead to carrier traps at oxide/semiconductor interfaces.[27] Nitrogen was found to prefer oxygen sites (N_O), acting as a source of negative fixed charge.[27]

Given the deleterious effects on device performance, passivation of these impurities could be highly fruitful. Hydrogen is known to act as an effective passivating agent for defects and impurities in many semiconductors and insulators.[28] Experiments have shown that annealing in H_2 or forming gas after the oxide deposition significantly improves the electrical properties of Ge, Si, and III-V-based MOS devices.[9,12−15,29] However, the microscopic mechanism behind this beneficial effect is still unclear. In this paper we investigate whether hydrogen is capable of passivating impurities in Al_2O_3.

We employ first-principles calculations to investigate the interaction between hydrogen and carbon or nitrogen impurities in Al_2O_3. Building on the results of ref 27 we assess the stability and change in electronic properties due to complex formation. We find that hydrogen forms stable complexes with both C and N. The electronic behavior is addressed by calculating charge-state transition levels and comparing them with the levels of isolated C and N impurities. These defect levels in Al_2O_3 can then be aligned with the band edges of the

Received: December 16, 2013
Accepted: February 26, 2014
Published: February 26, 2014

   dx.doi.org/10.1021/am4057997 | *ACS Appl. Mater. Interfaces* 2014, 6, 4149−4153

semiconductors using calculated band offsets, allowing an assessment of the impact of the defects on oxide/semiconductor interfaces. Such complexes are electrically inactive for Fermi-level positions near the semiconductor conduction bands, indicating effective passivation of the carbon-related carrier traps and the nitrogen-induced negative fixed charge centers.

COMPUTATIONAL APPROACH

Our calculations are based on density functional theory and the screened hybrid functional of Heyd–Scuseria–Ernzerhof (HSE),[30,31] implemented with the projector-augmented wave method[32] in the Vienna Ab initio Simulation Package (vasp) code.[33] The Hartree–Fock mixing parameter was set to 32%, resulting in a band gap of 9.2 eV for α-Al_2O_3. Impurity calculations were performed using periodic boundary conditions with supercells containing 120 atoms. The integrations over the Brillouin zone were performed using a $2 \times 2 \times 1$ k-point grid, and the electronic wave functions were expanded in a plane-wave basis set with an energy cutoff of 400 eV.

The formation energy of an impurity X in charge state q is given by[34]

$$E^f(X^q) = E_{tot}(X^q) - E_{tot}(Al_2O_3) - \sum_i n_i \cdot \mu_i + q \cdot \varepsilon_F + \Delta^q \quad (1)$$

where $E_{tot}(X^q)$ is the total energy of a supercell containing the impurity X in charge state q, and $E_{tot}(Al_2O_3)$ is the total energy of perfect Al_2O_3 in the same supercell. n_i is the number of atoms of type i added to or removed from the perfect crystal to form the defect, and μ_i is the respective atomic chemical potential. ε_F is the Fermi level referenced to the valence-band maximum (VBM), and Δ^q is the charge-state-dependent correction that contains the alignment of the electrostatic potentials of the bulk and defect supercells and accounts for errors due to the finite size of the supercell.[35,36]

The charge-state transition level (q/q') is defined as the Fermi-level position below which the defect is most stable in charge state q and above which the same defect is stable in charge state q'. It can be derived from formation energies as

$$(q/q') = \frac{E^f(X^q;\ \varepsilon_F = 0) - E^f(X^{q'};\ \varepsilon_F = 0)}{(q' - q)} \quad (2)$$

where $E^f(X^q;\ \varepsilon_F = 0)$ is the defect formation energy for charge state q when ε_F is at the VBM. The position of the transition level in the band gap does not depend on the chemical potentials.

The chemical potentials μ_i are referenced to the standard elemental phase of the species i; μ_{Al} is referenced to the total energy per atom of bulk Al; and the total energy per atom of an isolated O_2 molecule is taken as reference to μ_O. For the impurities, we take μ_H with respect to the energy per atom of the H_2 molecule, μ_N to that of the N_2 molecule, and μ_C to the energy per atom of diamond. To represent ALD growth conditions, we set $\mu_O = -0.65$ eV, corresponding to contact with O_2 gas at 270 °C and 1 Torr.

RESULTS AND DISCUSSION

Figure 1 shows the calculated formation energies of C–H and N–H complexes in Al_2O_3 as a function of Fermi level. For each Fermi-level position, we show only the formation energy of the lowest-energy charge state for each defect. The most stable configurations of the isolated C and N impurities, i.e., C_{Al} and N_O, are also included for comparison.[27] The charge-state transition levels (q/q') are shown as kinks in the curves of Figure 1.

Hydrogen Complex with Carbon. We find that the C_{Al}–H complex has lower formation energy than C_{Al} for virtually all Fermi-level positions; hydrogenation will thus result in the formation of such complexes. The (+2/0) transition level of C_{Al}–H occurs at 3.16 eV above the VBM and the (0/−2) level

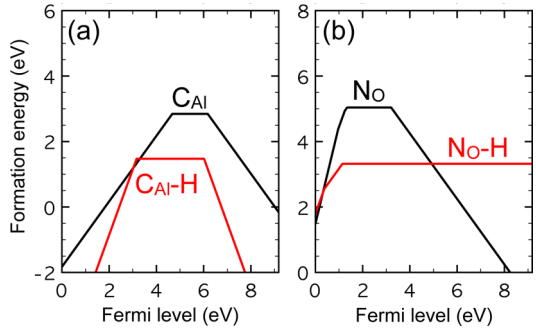

Figure 1. Formation energies as a function of Fermi level for (a) C_{Al}–H and (b) N_O–H complexes in Al_2O_3, for $\mu_O = -0.65$ eV. The Fermi level is referenced to the VBM of Al_2O_3. For comparison, the formation energies of the isolated C_{Al} and N_O impurities are also shown.

at 6.02 eV. The C_{Al}–H complex is thus neutral for 3.16 eV < ε_F < 6.02 eV; we will see that this is a very relevant energy range in the context of oxide/semiconductor interfaces.

As shown in Figure 2, C_{Al}–H can assume two distinct configurations. In the neutral charge state (Figure 2b), the

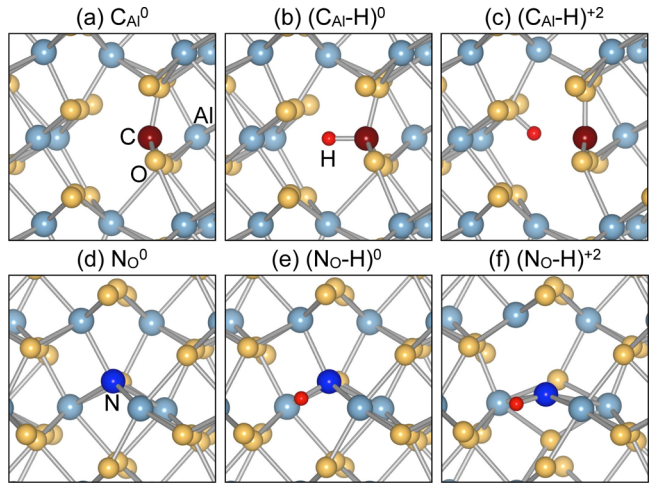

Figure 2. Ball-and-stick models of the structures of (a) neutral C_{Al}, (b) the C_{Al}–H complex in the neutral charge state, and (c) C_{Al}–H in the +2 charge state. The lower panels show the structure of (d) neutral N_O, (e) the N_O–H complex in the neutral charge state, and (f) N_O–H in the +2 charge state.

hydrogen atom prefers to bond to carbon with a C–H bond length of 1.04 Å. The three C–O bond lengths are 1.44 Å. In the +2 charge state (Figure 2c) the hydrogen atom bonds to a neighboring O atom with bond length of 0.97 Å, while the carbon atom becomes almost coplanar with three O neighbors, with C–O bond lengths of 1.28, 1.28, and 1.30 Å. The structure of $(C_{Al}–H)^{-2}$ is similar to that of $(C_{Al}–H)^0$.

Moving to the electronic structure, the single-particle energy states of C_{Al} and C_{Al}–H in the band gap are depicted in Figure 3. For neutral C_{Al} (Figure 3a), the singly occupied state lies 3.19 eV above the VBM, and an empty state occurs 8.07 eV above the VBM. In the +1 charge state (Figure 3b), an empty state is located at 6.37 eV. These states arise from a C dangling bond with p-orbital character. When the hydrogen atom is incorporated, H bonds to the carbon dangling bond, lowering the gap state to a position close to the VBM, at 0.76 eV. The state is occupied by two electrons.

dx.doi.org/10.1021/am4057997 | ACS Appl. Mater. Interfaces 2014, 6, 4149–4153

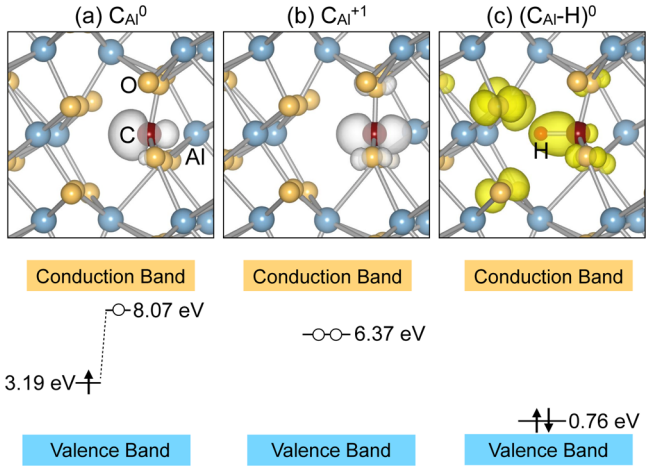

Figure 3. Charge density isosurfaces for the gap states of (a) neutral (C_{Al}^0), (b) singly positive (C_{Al}^{+1}), and (c) the neutral C−H complex (C_{Al}−H)^0. The charge densities of the highest gap state for each configuration are shown (white if the state is empty, yellow if occupied). The corresponding Kohn−Sham states in the band gap, along with their occupation, are also shown in the lower panels. The isosurfaces correspond to 10% of the maximum.[39]

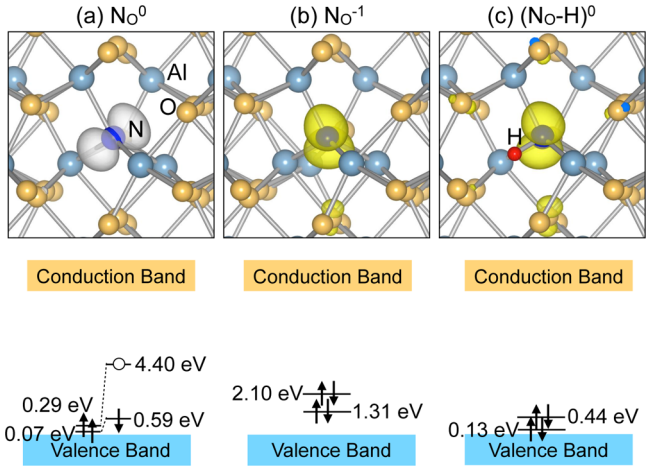

Figure 4. Charge density isosurfaces for the gap states of (a) neutral (N_O^0), (b) singly negative (N_O^{-1}), and (c) the neutral N−H complex (N_O−H)^0. The charge densities of the highest gap state for each configuration are shown (white if the state is empty, yellow if occupied). The corresponding Kohn−Sham states in the band gap, along with their occupation, are also shown in the lower panels. The isosurfaces correspond to 10% of the maximum.[39]

Hydrogen Complex with Nitrogen. Figure 1 shows that the N_O−H complex is electrically neutral for Fermi levels above 1.15 eV. A (+2/+1) transition level occurs at 0.38 eV and a (+1/0) level at 1.15 eV above the VBM. N_O−H has lower formation energy than N_O for $\varepsilon_F < 4.95$ eV. Note that annealing at higher H_2 pressures will result in lower formation energies for the complexes. In the neutral charge state (Figure 2e), H forms a N−H bond with a length of 1.02 Å, and the N−Al bond lengths are 1.88, 1.90, 2.00, and 2.01 Å. In the +2 charge state (Figure 2f), H is still bonded to the N atom, with a bond length of 1.02 Å; however, one of the N−Al bonds is broken, and N is bonded to three Al atoms with bond lengths of 1.92, 2.04, and 2.16 Å.

Figure 4 shows the single-particle states for N_O and N_O−H in the band gap. For N_O^0 (Figure 4a), singly electron occupied states are found at 0.07 and 0.29 eV (spin-up) and 0.59 eV (spin-down) above the VBM. An empty state occurs 4.40 eV above the VBM in the spin-down channel. In the −1 charge state (Figure 4b), two states occur at 1.31 and 2.10 eV. These states arise from a N p-like orbital. For the N_O−H complex, hydrogen bonds to the N atom, introducing two occupied states at 0.13 and 0.44 eV, i.e., slightly above the VBM. In contrast to the C_{Al}−H complex, these states do not have density on the hydrogen atom.

Impact of H Complexes on Al_2O_3 Gate Dielectrics in MOS Devices. The kinks in the curves in Figure 1 delineate the regions of stability of different charge states and correspond to the impurity levels that would be experimentally observed in the oxide. On the right-hand side of Figure 5 we depict that information for the impurities and their complexes, with the impurity levels shown within the band gap of Al_2O_3. To examine the impact of these impurities and complexes on the electrical properties of devices, we need to figure out how the impurity levels are aligned with the band structures of the semiconductors on which the oxide is deposited. We can obtain such an alignment by using calculated band offsets between the semiconductors and Al_2O_3.

To examine band offsets between Al_2O_3 and GaN, we performed a bulk calculation for each material to obtain the

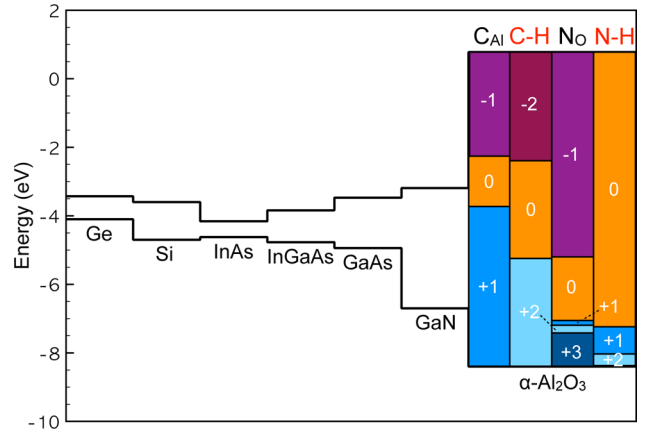

Figure 5. Band alignment between semiconductors (Ge, Si, III-As, GaN) and Al_2O_3. For each material, the lower line corresponds to the VBM and the upper line to the CBM. The composition of the InGaAs alloy is $In_{0.53}Ga_{0.47}As$, corresponding to lattice matching to InP. Stable charge states and the position of charge-state transition levels for C and N impurities and their complexes with hydrogen are shown within the oxide band gap. The zero was set at the vacuum level.

band edges relative to the averaged electrostatic potential and a slab calculation to obtain the position of the averaged electrostatic potential in the bulk with respect to the vacuum.[17] By combining bulk and slab calculations, we find the position of the band edges relative to the vacuum level. The calculated valence-band offset is 1.7 eV, in good agreement with the experimental value of 1.8 eV.[37] The band-edge positions of GaN, III-As, Si, and Ge with respect to the vacuum level were taken from ref 38. The resulting valence-band offsets with Al_2O_3 are 3.8 eV for InAs, 3.5 eV for GaAs, 3.6 eV for $In_{0.53}Ga_{0.47}As$, 3.7 eV for Si, and 4.3 eV for Ge.

Actual devices will exhibit deviations from the flat-band conditions depicted in Figure 5, due to space-charge regions in the semiconductor or electric fields in the dielectric. However, the natural band alignment between the materials is an interface-specific property and correctly described by the values

dx.doi.org/10.1021/am4057997 | ACS Appl. Mater. Interfaces 2014, 6, 4149−4153

depicted in Figure 5. The positions of impurity levels with respect to the semiconductor band edges in the vicinity of the interface are thus correctly given. The electrical activity of impurities may change depending on the position of their levels with respect to the Fermi level, but those effects will be correctly described if band bending in the semiconductor and the presence of any electric field in the dielectric are taken into account in a device simulation.

The behavior of C and its complex with hydrogen is similar for the interfaces between Al_2O_3 and all the III-V semiconductors discussed here, in the case of *n*-type devices in which the Fermi level lies near the CBM of the semiconductor. The (+1/0) level of the isolated C_{Al} impurity lies in the vicinity of the CBM of the III-V semiconductors (0.54 eV below the CBM of GaN, 0.11 eV above the CBM of $In_{0.53}Ga_{0.47}As$), indicating that carbon behaves as a source of border traps or bulk traps.[25−27] Hydrogenation removes this level from the vicinity of the semiconductor CBM: in the case of GaN the (0/−2) level of C_{Al}−H lies 0.81 eV above the GaN CBM and the (+2/0) level 2.05 eV below the CBM; in the case of InGaAs, the (0/−2) level lies 1.46 eV above the $In_{0.53}Ga_{0.47}As$ CBM and the (+2/0) level 0.47 eV below the $In_{0.53}Ga_{0.47}As$ VBM. C_{Al}−H is therefore electrically inactive near the Al_2O_3/*n*-GaN and Al_2O_3/*n*-$In_{0.53}Ga_{0.47}As$ interface, indicating that hydrogen effectively passivates C impurities.

In the case of nitrogen, the (0/−1) transition level associated with N_O in Al_2O_3 lies well below the CBM of all of the semiconductors, and hence nitrogen behaves as a negative fixed-charge center.[27] Upon hydrogenation, the N_O−H complex is neutral over the entire range of Fermi levels within the band gaps of the semiconductors considered here, thus removing the source of fixed charge. In ref 27 it was noted that nitrogen can play a beneficial role in Al_2O_3 because its incorporation as N_O, in oxygen-deficient material, suppresses the formation of carrier traps associated with oxygen vacancies. This is at the expense, however, of forming negative fixed charge centers, which are also undesirable. Here we have shown that hydrogenation (for instance, by annealing in forming gas) additionally removes this fixed charge since it leads to electrically neutral N_O−H complexes.

Regarding Ge and Si MOS structures, the isolated C_{Al} can be a carrier trap, since the (+1/0) level of the isolated C_{Al} impurity lies in the vicinity of the CBM of the semiconductors (0.30 eV below the Ge CBM, 0.13 eV below the Si CBM). Again, hydrogenation removes this level from the vicinity of the semiconductor CBM: in the case of Ge the (0/−2) level of C_{Al}−H lies 1.05 eV above the Ge CBM and the (+2/0) level 1.81 eV below the CBM; in the case of Si, the (0/−2) level occurs 1.22 eV above the Si CBM and the (+2/0) level 1.64 eV below the Si VBM. Thus, C_{Al}−H is electrically inactive near the *n*-Ge and *n*-Si interface with Al_2O_3, indicating that hydrogen effectively passivates carbon-associated traps.

Hydrogen passivation appears to be somewhat less effective in the case of interfaces between Al_2O_3 and *p*-type semiconductors, in which the Fermi level lies near the semiconductor VBM. The (+2/0) level of the C_{Al}−H complex lies only 0.30 eV below the VBM of GaAs, indicating that it might still act as a carrier trap, and for *p*-GaN, the C_{Al}−H complex occurs in the +2 charge state and thus acts as a source of positive fixed charge. The N−H complex is neutral and inert in the case of interfaces with III-arsenides, Ge, and Si, but its (+1/0) level lies near the VBM of GaN and could potentially act as a carrier trap.

CONCLUSIONS

We have performed hybrid functional calculations to study carbon and nitrogen impurities in Al_2O_3 and their passivation by hydrogen. Carbon and nitrogen are often contained in precursors used as metal or oxygen sources, and they are likely to incorporate into the deposited dielectrics. We find that hydrogen eliminates carrier traps caused by carbon and removes negative fixed charge caused by nitrogen impurities. Hydrogen is thus an effective passivating agent, at least for *n*-type MOS devices based on Al_2O_3/semiconductor (Ge, Si, III-As, GaN).

AUTHOR INFORMATION

Corresponding Author

*E-mail: minseokchoi.phd@gmail.com.

Notes

The authors declare no competing financial interest.

ACKNOWLEDGMENTS

M.C. was supported by the ONR DEFINE MURI (N00014-10-1-0937). A.J. was supported by the U.S. Army Research Office (W911-NF-11-1-0232). Computational resources were provided by the Center for Scientific Computing at the CNSI and MRL: an NSF MRSEC (DMR-1121053) and by XSEDE (NSF OCI-1053575 and DMR07-0072N).

REFERENCES

(1) Liu, L.; Edgar, J. Substrates for Gallium Nitride Epitaxy. *Mater. Sci. Eng., R* **2002**, *37*, 61−127.

(2) Wang, W.; Wang, S.; Ma, X.; Gong, J. Recent Advances in Catalytic Hydrogenation of Carbon Dioxide. *Chem. Soc. Rev.* **2011**, *4*, 3703−3727.

(3) Dingemans, G.; Kessels, W. M. M. Status and Prospects of Al_2O_3-Based Surface Passivation Schemes for Silicon Solar Cells. *J. Vac. Sci. Technol., A* **2012**, *30*, 040802.

(4) Akselrod, M. S.; Bruni, F. J. Modern Trends in Crystal Growth and New Applications of Sapphire. *J. Cryst. Growth* **2012**, *360*, 134−145.

(5) Mishra, U. K.; Shen, L.; Kazior, T.; Wu, Y.-F. GaN-Based RF Power Devices and Amplifiers. *Proc. IEEE* **2008**, *96*, 287−305.

(6) Oktyabrsky, S.; Ye, P. D., Eds. *Fundamentals of III-V Semiconductor MOSFETs*; Springer: New York, 2010.

(7) Long, R. D.; McIntyre, P. C. Surface Preparation and Deposited Gate Oxides for Gallium Nitride Based Metal Oxide Semiconductor Devices. *Materials* **2012**, *5*, 1297−1335.

(8) Wallace, R. M.; McIntyre, P. C.; Kim, J.; Nishi, Y. Atomic Layer Deposition of Dielectrics on Ge and III-V Materials for Ultrahigh Performance Transistors. *MRS Bull.* **2009**, *34*, 493−503.

(9) Swaminathan, S.; Shandalov, M.; Oshima, Y.; McIntyre, P. C. Bilayer Metal Oxide Gate Insulators for Scaled Ge-Channel Metal-Oxide-Semiconductor Devices. *Appl. Phys. Lett.* **2010**, *96*, 082904.

(10) Chang, Y. C.; Chang, W. H.; Chiu, H. C.; Tung, L. T.; Lee, C. H.; Shiu, K. H.; Hong, M.; Kwo, J.; Hong, J. M.; Tsai, C. C. Inversion-Channel GaN Metal-Oxide-Semiconductor Field-Effect Transistor with Atomic-Layer-Deposited Al_2O_3 as Gate Dielectric. *Appl. Phys. Lett.* **2008**, *93*, 053504.

(11) Nepal, N.; Garces, N. Y.; Meyer, D. J.; Hite, J. K.; Mastro, M. A.; Eddy, C. R., Jr. Assessment of GaN Surface Pretreatment for Atomic Layer Deposited High-*k* Dielectrics. *Appl. Phys. Express* **2011**, *4*, 055802.

(12) Zafar, S.; Callegari, A.; Narayanan, V.; Guha, S. Impact of Moisture on Charge Trapping and Flatband Voltage in Al_2O_3 Gate Dielectric Films. *Appl. Phys. Lett.* **2002**, *81*, 2608−2610.

(13) Shin, B.; Weber, J. R.; Long, R. D.; Hurley, P. K.; Van de Walle, C. G.; McIntyre, P. C. Origin and Passivation of Fixed Charge in

Atomic Layer Deposited Aluminum Oxide Gate Insulators on Chemically Treated InGaAs Substrates. *Appl. Phys. Lett.* **2010**, *96*, 152908.
(14) Kim, E. J.; Wang, L.; Asbeck, P. M.; Saraswat, K. C.; McIntyre, P. C. Border Traps in $Al_2O_3/In_{0.53}Ga_{0.47}As$ (100) Gate Stacks and Their Passivation by Hydrogen Anneals. *Appl. Phys. Lett.* **2010**, *96*, 012906.
(15) Hu, J.; Wong, H.-S. P. Effect of Annealing Ambient and Temperature on the Electrical Characteristics of Atomic Layer Deposition $Al_2O_3/In_{0.53}Ga_{0.47}As$ Metal-Oxide-Semiconductor Capacitors and MOSFETs. *J. Appl. Phys.* **2012**, *111*, 044105.
(16) Weber, J. R.; Janotti, A.; Van de Walle, C. G. Native Defects in Al_2O_3 and Their Impact on III-V/Al_2O_3 Metal-Oxide-Semiconductor-Based Devices. *J. Appl. Phys.* **2011**, *109*, 033715.
(17) Choi, M.; Janotti, A.; Van de Walle, C. G. Native Point Defects and Dangling Bonds in a-Al_2O_3. *J. Appl. Phys.* **2013**, *113*, 044501.
(18) Van de Walle, C. G.; Choi, M.; Weber, J.; Lyons, J.; Janotti, A. Defects at Ge/Oxide and III-V/Oxide Interfaces. *Microelectron. Eng.* **2013**, *109*, 211−215.
(19) Puurunen, R. L. Surface Chemistry of Atomic Layer Deposition: A Case Study for the Trimethylaluminum/Water Process. *J. Appl. Phys.* **2005**, *97*, 121301.
(20) Liu, X.; Ramanathan, S.; Longdergan, A.; Srivastava, A.; Lee, E.; Seidel, T.; Barton, J.; Pang, D.; Gordon, R. AID of Hafnium Oxide Thin Film from Tetrakis(ethylmethylamino)hafnium and Ozone. *J. Electrochem. Soc.* **2005**, *152*, G213−G219.
(21) Miikkulainen, V.; Leskela, M.; Ritala, M.; Puurunen, R. L. Crystallinity of Inorganic Films Grown by Atomic Layer Deposition: Overview and General Trends. *J. Appl. Phys.* **2013**, *113*, 021301.
(22) Cho, M.; Jeong, D. S.; Park, J.; Park, H. B.; Lee, S. W.; Park, T. J.; Hwang, C. S.; Jang, G. H.; Jeong, J. Comparison between Atomic-Layer-Deposited HfO_2 Films Using O_3 or H_2O Oxidant and $Hf[N(CH_3)_2]_4$ Precursor. *Appl. Phys. Lett.* **2004**, *85*, 5953.
(23) Cho, M.; Kim, J. H.; Hwang, C. S.; Ahn, H.-S.; Han, S.; Won, J. Y. Effects of Carbon Residue in Atomic Layer Deposited HfO_2 Films on Their Time-Dependent Dielectric Breakdown Reliability. *Appl. Phys. Lett.* **2007**, *90*, 182907.
(24) Mazumder, B.; Esposto, M.; Hung, T. H.; Mates, T.; Rajan, S.; Speck, J. S. Characterization of a Dielectric/GaN System Using Atom Probe Tomography. *Appl. Phys. Lett.* **2013**, *103*, 151601.
(25) Liu, X.; Yeluri, R.; Kim, J.; Lal, S.; Raman, A.; Lund, C.; Wienecke, S.; Lu, J.; Laurent, M.; Keller, S.; Mishra, U. K. In-Situ Metalorganic Chemical Vapor Deposition and Capacitance-Voltage Characterizations of Al_2O_3 on Ga-Face GaN Metal-Oxide-Semiconductor Capacitors. *Appl. Phys. Lett.* **2013**, *103*, 053509.
(26) Liu, X.; Kim, J.; Yeluri, R.; Lal, S.; Li, H.; Lu, J.; Keller, S.; Mazumder, B.; Speck, J. S.; Mishra, U. K. Fixed Charge and Trap States of In Situ Al_2O_3 on Ga-Face GaN Metal-Oxide-Semiconductor Capacitors Grown by Metalorganic Chemical Vapor Deposition. *J. Appl. Phys.* **2013**, *114*, 164507.
(27) Choi, M.; Lyons, J. L.; Janotti, A.; Van de Walle, C. G. Impact of Carbon and Nitrogen Impurities in High-κ Dielectrics on Metal-Oxide-Semiconductor Devices. *Appl. Phys. Lett.* **2013**, *102*, 142902.
(28) Van de Walle, C. G.; Neugebauer, J. Hydrogen in Semiconductors. *Annu. Rev. Mater. Res.* **2006**, *36*, 179.
(29) Hung, T.-H.; Krishnamoorthy, S.; Esposto, M.; Nath, D. N.; Park, P. S.; Rajan, S. Interface Charge Engineering at Atomic Layer Deposited Dielectric/III-nitride Interfaces. *Appl. Phys. Lett.* **2013**, *102*, 072105.
(30) Heyd, J.; Scuseria, G. E.; Ernzerhof, M. Hybrid Functionals Based on a Screened Coulomb Potential. *J. Chem. Phys.* **2003**, *118*, 8207−8215.
(31) Krukau, A. V.; Vydrov, O. A.; Izmaylov, A. F.; Scuseria, G. E. Influence of the Exchange Screening Parameter on the Performance of Screened Hybrid Functionals. *J. Chem. Phys.* **2006**, *125*, 224106.
(32) Blöchl, P. E. Projector Augmented-Wave Method. *Phys. Rev. B* **1994**, *50*, 17953−17979.
(33) Kresse, G.; Hafner, J. Ab Initio Molecular Dynamics for Open-Shell Transition Metals. *Phys. Rev. B* **1993**, *48*, 13115.
(34) Van de Walle, C. G.; Neugebauer, J. First-Principles Calculations for Defects and Impurities: Applications to III-Nitrides. *J. Appl. Phys.* **2004**, *95*, 3851−3879.
(35) Freysoldt, C.; Neugebauer, J.; Van de Walle, C. G. Fully *Ab Initio* Finite-Size Corrections for Charged-Defect Supercell Calculations. *Phys. Rev. Lett.* **2009**, *102*, 016402.
(36) Freysoldt, C.; Neugebauer, J.; Van de Walle, C. G. Electrostatic Interactions between Charged Defects in Supercells. *Phys. Status Solidi B* **2011**, *248*, 1067−1076.
(37) Yang, J.; Eller, B. S.; Zhu, C.; England, C.; Nemanich, R. J. Comparative Band Alignment of Plasma-Enhanced Atomic Layer Deposited high-k Dielectrics on Gallium Nitride. *J. Appl. Phys.* **2012**, *112*, 053710.
(38) Van de Walle, C. G.; Neugebauer, J. Universal Alignment of Hydrogen Levels in Semiconductors, Insulators and Solutions. *Nature* **2003**, *423*, 626.
(39) Momma, K.; Izumi, F. *VESTA3* for Three-Dimensional Visualization of Crystal, Volumetric and Morphology Data. *J. Appl. Crystallogr.* **2011**, *44*, 1272−1276.